Wylie, D., W. Wolf, P. Piironen, E. Eloranta, "Visible infrared optical depths of cirrus as seen by satellite and scanning lidar", Cloud Impact on Defence Operations and Systems, Fort Belvoir, Virginia, November 15-19, 1993.

VISIBLE/INFRARED OPTICAL DEPTHS OF CIRRUS AS SEEN BY SATELLITE AND SCANNING LIDAR

Donald Wylie, Walt Wolf, Paivi Piironen and Edwin Eloranta

University of Wisconsin-Madison
Madison, WI 53706

57-47
71210

1. INTRODUCTION

A large body of cloud statistics have been recently compiled from satellite data, Schiffer and Rossow, (1983) and Wylie and Menzel, (1993). These are from infrared satellite sensors which can be added to the CFLOS data base which came primarily from visual observations. To quantitatively use the satellite data, the relationship between the visible and infrared optical depths of the clouds must be established. To study this relationship, we combined data of the visible scattering in cirrus from lidars with infrared emittance and transmission data from satellites.

Previous studies of the visible and IR radiative properties of ice clouds have been made by Platt (1979) using lidar with an IR radiometer and Minnis et al. (1990) using satellite and lidar data from a case study in FIRE. Platt (1979) collected several cases of cirrus clouds and found a ratio of the visible/IR optical depths of 2:1. The Minnis et al. (1990) FIRE case study found the visible/IR ratio to be slightly higher, 2.1:1. Modelling of radiative properties of ice crystals suggest that the visible/IR ratio can vary from 1.8 to 4.0 (Minnis et al., 1993).

The previous studies have been limited in scope because of the difficulty in obtaining visible and IR data together. To expand our knowledge of the visible and IR radiative properties of transmissive cirrus, we initiated our own study.

One of the largest problems for any cirrus cloud study is the large spatial variability of clouds. Vertically pointing lidars sample only the part of the cloud that drifted over them. They have a vary narrow beam, < 1 m in width. Satellites can see spatial gradients in clouds but have less resolution. Satellite radiometer field of views (FOV) vary from 1 to 20 km. To reduce the spatial sampling problem caused by this mix of instruments, a scanning lidar was used to make volume imagery of cirrus clouds similar to the satellite view of the same clouds.

2. MEASUREMENT TECHNIQUE

The High Spectral Resolution Lidar (HSRL) and the Volume Imaging Lidar (VIL) of the University of Wisconsin-Madison were combined to produce a quantitative image of the visible optical depth of cirrus clouds. The HSRL is a unique instrument that measures the extinction and optical depth of the cloud without assuming the extinction to backscatter ratio in clouds. Simple lidars require estimating extinction from the backscattered return measured by the lidar. The extinction to backscatter ratio varies depending on the constituents of the clouds. The HSRL directly measurements this radiative property of the clouds. Details of this system are given else where in these proceedings by Eloranta et al., (1993).

To understand radiative scattering in clouds, the large horizontal and vertical variations in cloud structure have to be measured. The HSRL samples only a small portion of the cloud - a column about 30 centimeters wide. The GOES satellite IR sensors have a horizontal resolution of 10.8 km at Madison, WI. To account for FOV differences, the horizontal structure of the clouds were measured by the VIL.

The VIL produced visible backscatter images of the clouds by scanning across the wind (see Figure 1). Time advection of the clouds was used to construct a horizontal image of visible backscatter from the VIL data over a one hour period. An example is shown in Figure 2. This image covers 100 km in the north-south direction. The location of the VIL is the center of the image. The image is skewed because it has been distorted to the projection of the GOES satellite image.

The HSRL was used to calibrate the VIL signal into backscatter cross sections of particulates. The backscatter cross sections were related to extinction by a constant backscatter phase function determined from the HSRL data. This process produced a three dimensional image of visible extinction in the cirrus clouds over a one hour period.

The extinction volume image was then transformed to an image of optical depth in the same viewing geometry as the GOES satellite (Fig. 2). Optical depths were formed from the integral of extinction along the path in which the GOES scanner viewed this volume. The optical depth image was originally produced with a 1 km (satellite nadir) resolution. This image was then shifted to align with the satellite IR image to account for error in the satellite registration system. The lidar visible optical depth image then was averaged to an 8 km (satellite nadir) image for direct comparison to the satellite IR image. This gave coincident fields of views from both satellite and lidars in the same geometry with a horizontal resolution of 10.8 km per pixel.

IR optical depths were extracted from the GOES image using calculations of the IR transmittance of the clouds using the IR radiance of the cloud, the radiance of cloud free FOV's and radiances calculated from the temperature of the mean vertical level of the cloud. The VIL data were used to determine the cloud level. Rawinsonde observations were made at Madison at the same time as these data.

All dual lidar data were taken in the vicinity of Madison, WI on 1 December, 1989. The VIL was located 24 km west of the HSRL. The VIL scanned both crosswind and nearly downwind over the HSRL. Data were taken from 19:35 UTC (13:35 Local) to 21:20 UTC (15:20 L). During this time a large mass of cirrus clouds moved into the region from the west-northwest with an approaching cold front. Madison, WI was under cloud free sky during the morning and proceeded to total overcast by the end of this period. Two lidar images were constructed from 1 hour VIL crossection records. More details on the data taken can be found in Ackerman et al. (1993).

3. RESULTS

An example of the cirrus cloud structure viewed by the VIL is shown in Figure 1. A thick cloud mass from 6.8 to 9.0 km is apparent from 8 km south to 20 km north of the VIL. Other thin broken layers are apparent both north and south of the large mass. This is typical of the different forms of cirrus sampled on 1 Dec, 89. The first clouds to reach Madison were vertically thin and horizontally broken. A few dense lines with evidence of precipitating virga also were found in the VIL volume. Later thicker cirrus moved in with virga that spanned the 2.2 km shown in Fig. 1.

The satellite and VIL images were divided into regions of similar cloud characteristics. The VIL cross sections were used as the primary division tool. The GOES image had little detail in the IR, although the same general spatial pattern as the lidar image was seen. The lidar visible optical depth image at 1 km showed many line and sheet structures. Cloud thickness, the presence of multiple layers and the intensity of precipitating virga were used to segregate different cloud forms.

The visible and accompanying IR optical depths are shown in Fig. 3. Most of the data are near the 2:1 line shown in the image. These data loosely agree with theory and the other past measurements. However, the visible/IR optical depth ratio appears to increase for thicker precipitating cirrus. Clouds with dense precipitating virga have ratios below the 2:1 line (visible/IR > 2). Cloud areas of highest reflectivity had solid lidar returns over 2 km depth with occasional embedded layers of extremely high reflectivity. The horizontal variations in cloud reflectivity were seen in the IR satellite imagery but with far less detail than the lidar images. The lower resolution of the satellite IR sensor smoothed some of these variations. However, the lidar data show that visible reflectivity had a wide range of values with large vertical and horizontal detail.

More data have been added to Fig. 3 from 1993. HSRL data have been taken during polar orbiter NOAA satellite passes over Madison, WI. The VIL was not used with these data. An example of HSRL data from 12 October 93 is shown in Figure 4. NOAA 12 crossed the HSRL at 00:36 (UTC). The IR image is shown in Figure 5. Light cirrus from 7.8 to 10.5 km moved over the HSRL before the NOAA 12 overpass.

Some bright cells were apparent in the HSRL data (Fig. 4) that could not be seen in the NOAA 12 IR image (Fig. 5). The scanning resolution of the NOAA 12 image was 1 km (HRPT) and has been remapped to a rectangular latitude-longitude coordinate projection. It appears that the bright cells apparent in the HSRL time section, are smoothed over in the satellite IR image.

A time record of the optical depth of this cloud measured by the HSRL is shown in Figure 6. The optical depth was very low, around 0.1 before the cirrus arrived. At about 0:06 UTC (0.1 decimal hour on absissa), the optical depth radically increased to 1.15 and then decreased to 0.9 at the time of the satellite overpass. Later, the visible optical depths dropped into a range from 0.25 to 0.6.

Also shown on Fig. 6 are equivalent IR optical depths taken from the satellite image. The spatial satellite image was converted to a time section using the wind at 9 km.

Some discrepancies between the satellite and the lidar optical depths are apparent. The large visible optical depth measured at 0.35 UTC by the lidar, 0.25 hour before the satellite overpass, did not appear in the satellite image. The satellite measured nearly consistent temperatures around 262 K. Later the satellite image follows the lidar time section with optical depths dropping at 1.35 UTC.

The cirrus was evaporating as it crossed the HSRL from the northwest. It appears that the intense cells that appeared in the HSRL time record decayed down wind by the time of the satellite overpass. These cells lasted for 0.1 hour over the lidar. The 9 km wind speed was 22.7 km/hr. This implies that the cells were at least 2.2 km long in the down wind direction which should have been visible on the 1 km satellite image. The cross wind scans of the VIL would have been useful in determining the areal coverage of these cells.

The HSRL and NOAA satellite data are shown on Fig 3. They fall near the 2:1 line inside the points taken from the HSRL, VIL and GOES data from 1 December 89.

4. CONCLUSION

These data appear to confirm the previous studies of Platt (1979) and Minnis et al. (1990). The visible/IR optical depth ratios have been in the range of 1:1 to 4:1.

The strength of the precipitating virga definitely affected the visible/IR optical depth ratio. This ratio was found to $\leq$ 2:1 for clouds with weak or no virga. While cirrus with dense virga had ratio's of > 2:1.

Some other trends are being investigated. The presence of water at the top of cirrus layers has been found in the 1993 data. The HSRL can identify water from ice by polarization measurements that have recently been added. These data have not been shown here, but are under study and the effects of water on the visible/IR optical depth will be reported at some later date.

There is a slight indication that the temperature of the cloud has some effect on the visible/IR optical depth ratio. The clouds studied in 1989 were warmer and of lower altitude than the 1993 data. The recently acquired data lack any points with visible/IR ratios > 2:1. We will look for this trend with future data.

5. REFERENCES

Ackerman, S. A., E. W. Eloranta, C. J. Grund, R. O. Knuteson, H. E. Revercomb, W. L. Smith and D. P. Wylie, 1993: University of Wisconsin Remote Sensing Pilot Experiment. Bull. A.M.S.

Eloranta, E.W., and P. Piironen, 1993: Remote measurements of cloud optical properties with a robust high spectral resolution lidar., CIDOS-93.

Minnis, P., D.F. Young, K. Sassen, J.M. Alvarez and C.J. Grund, 1990: The October 27-28 1986 FIRE IFO Cirrus Case Study: Cirrus parameter relationships derived from satellite and lidar data. Mon. Wea. Rev., 118, 2402 2425.

Minnis, P., K.N. Liou and Y. Takano, 1993: Inference of cirrus cloud properties using satellite-observed visible and infrared radiances. Part I: Parameterization of radiance fields, J. Atm. Sci., 50, 1279-1304.

Platt, C.M.R., 1979: Remote sounding of high clouds, I: Calculations of visible and infrared optical properties from lidar and radiometer measurements., J. Appl. Meteor., **18**, 1130-1143.

Schiffer, R.A. and W.B. Rossow, 1983: The International Satellite Cloud Climatology Project (ISCCP): The first project of the World Climate Research Programme., Bull. Amer. Meteor. Soc., 64, 779-784.

Wylie, D.P. and W.P. Menzel, 1993: Four years of global cirrus cloud statistics using HIRS., Submitted to J. Climatology.

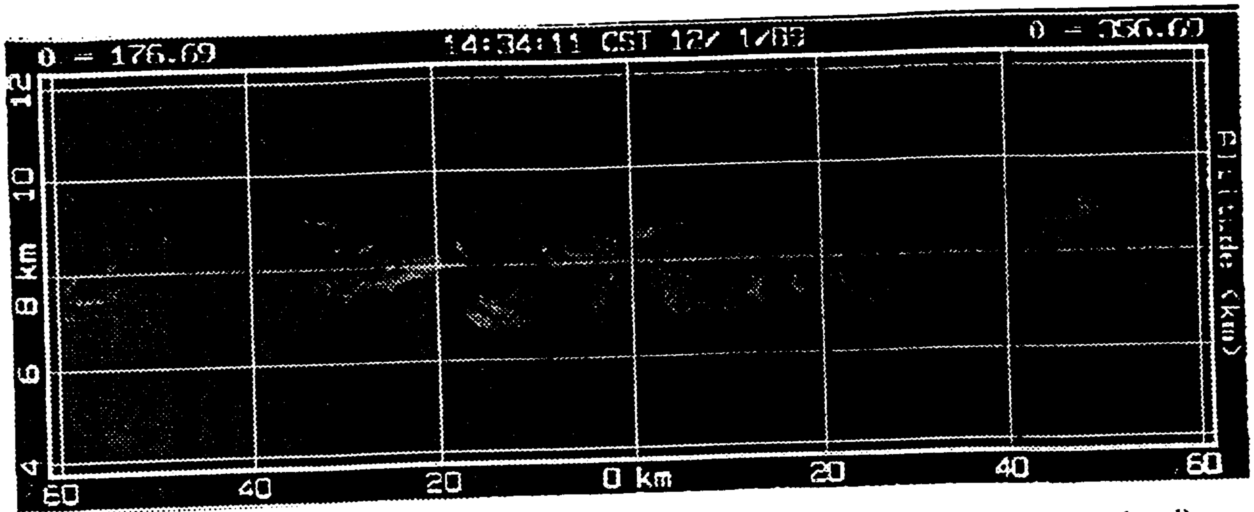

Figure 1: A Volume Imaging Lidar (VIL) cross wind section taken at 20:34 UTC (14:34 local). Scan directions were azimuths of 177° and 357°. Orientation is south to north.

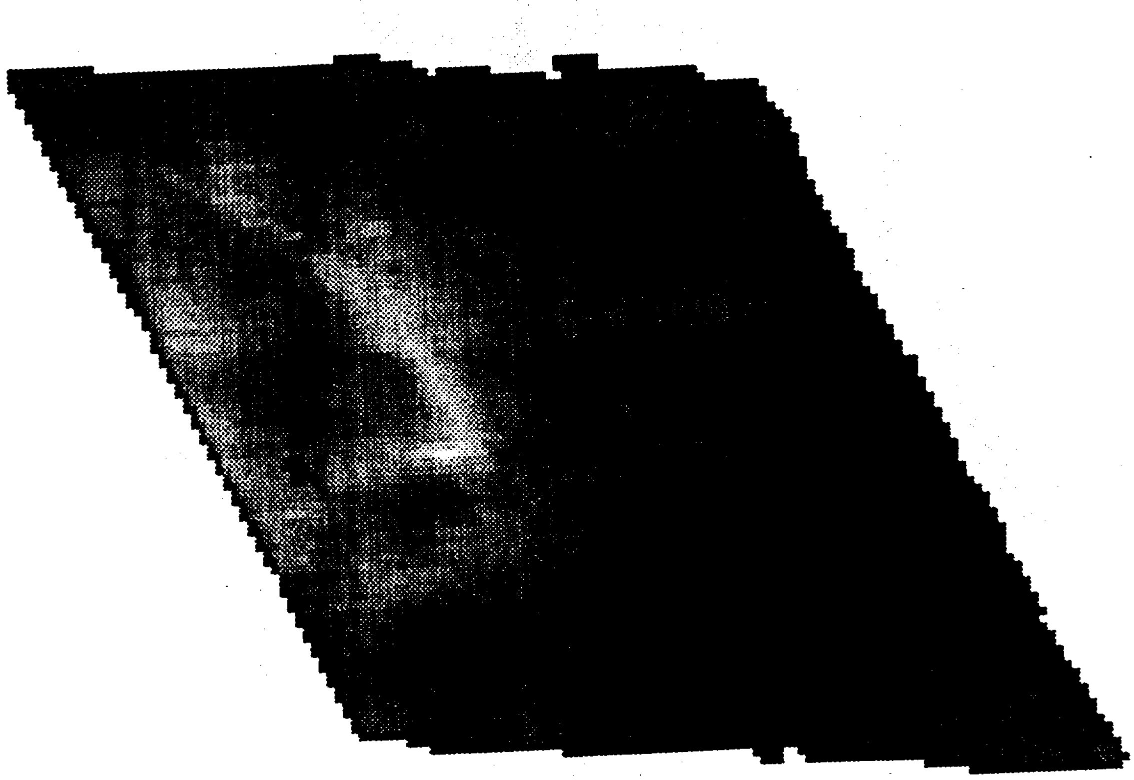

Figure 2: An image in the projection of the GOES satellite made from the cross wind scans of the VIL from 20:35 to 21:20 UTC, 1 December 1989. The VIL scan in Fig. 1 is near the center of the image. Boundaries of the image are north-south and east-west.

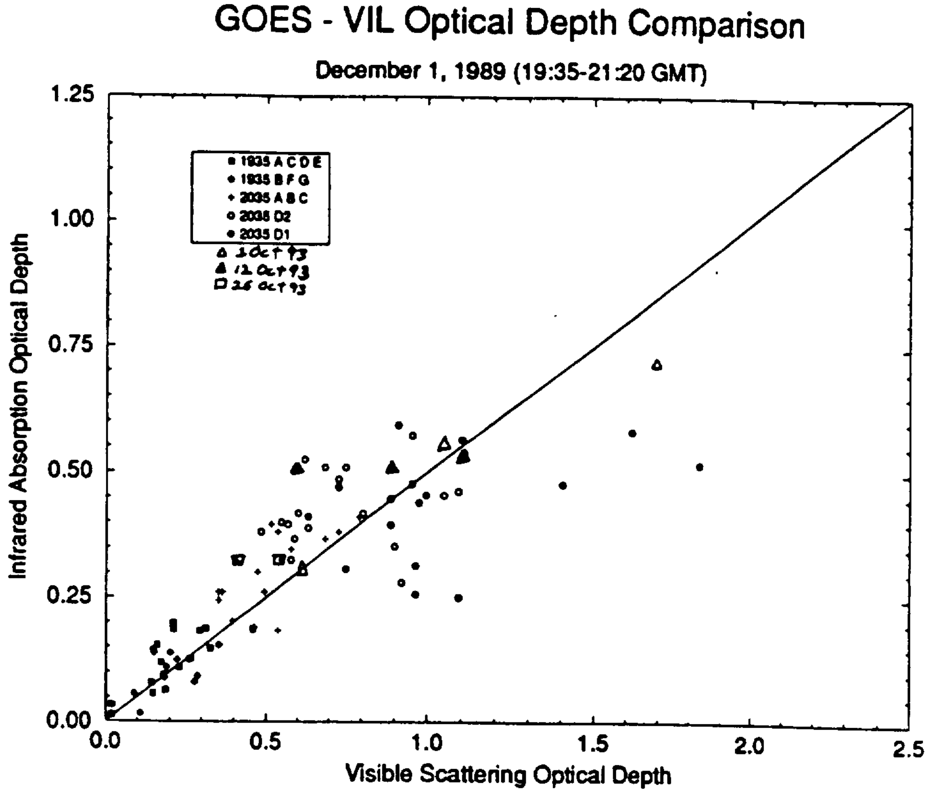

Figure 3: Scatter plot of the visible and IR optical depths of cirrus clouds using coincident lidar and satellite data.

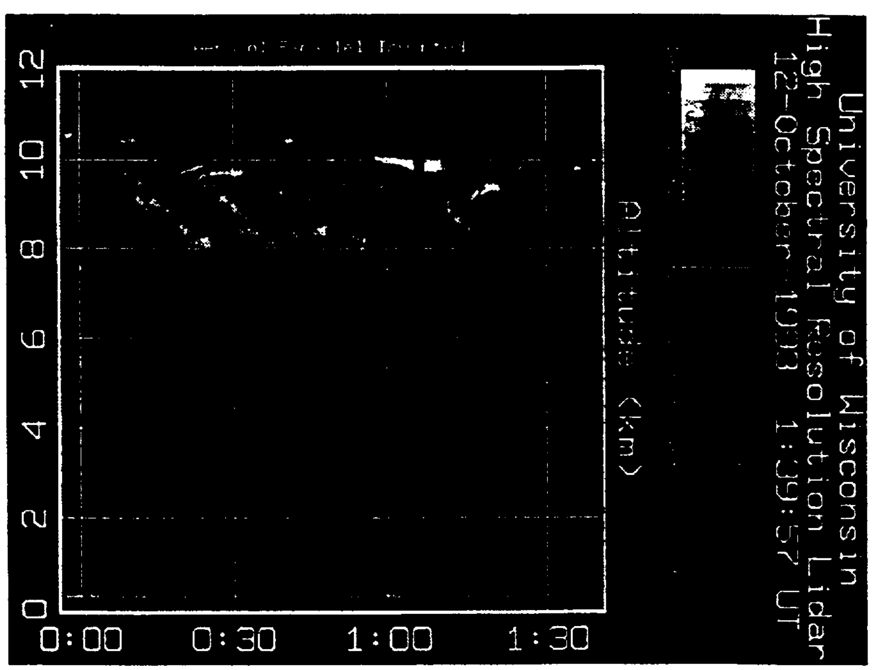

Figure 4: Time section of the HSRL lidar taken at Madison, WI on 12 October 93. The time scale is UTC.

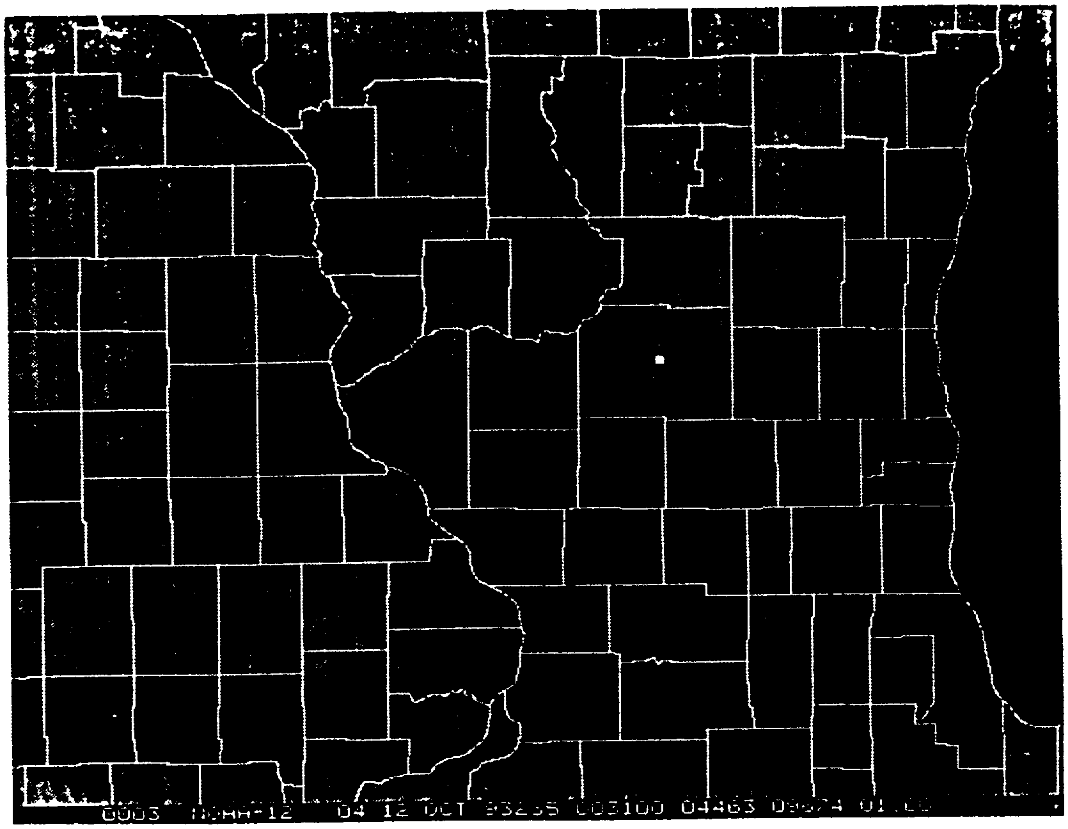

Figure 5: The NOAA 12 AVHRR HRPT channel 4 (11 micron) infrared image from 00:36 UTC, 12 October 93. This image has been rectified to an equal distance latitude-longitude projection.

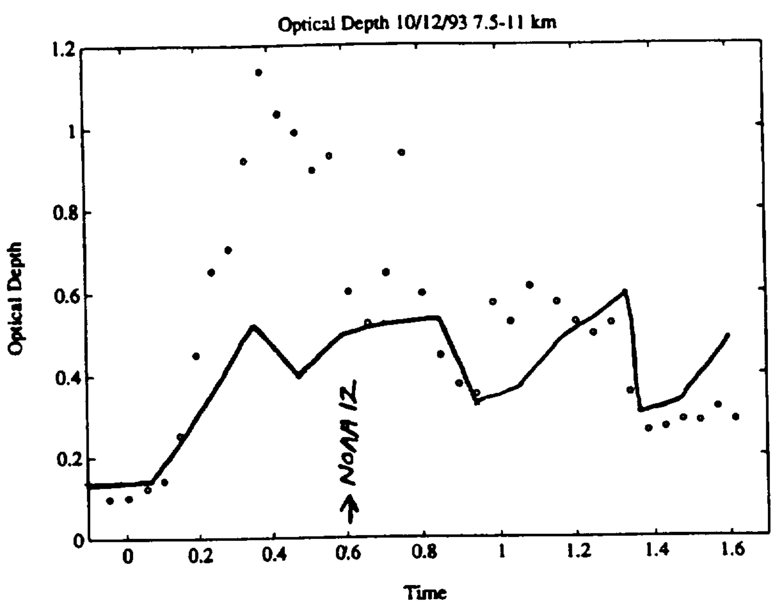

Figure 6: The optical depths measured by the HSRL on 12 October 93 (circles) and the from the NOAA 12 image (solid line).